Springer

RARE METALS

Supporting Information

Three-dimensional CeO_2@carbon-quantum-dots scaffold modified with Au nanoparticles on flexible substrates for high performance gas sensing at room temperature

Chao Wang*, Long Zhang, Bing He, Quan Zhou, Shao-Hui Zhang, Xiu-Li Kong, Zhen Chen, Ge-Bo Pan*

C. Wang*, X.-L. Kong, Z.Chen
School of Chemistry and Pharmaceutical Engineering, Shandong First Medical University & Shandong Academy of Medical Sciences, Tai'an 271016, China
e-mail: chaowang2017@sinano.ac.cn

L. Zhang, Q. Zhou, G.-B. Pan*
Division of Interdisciplinary and Comprehensive Research, Suzhou Institute of Nano-Tech and Nano-Bionics, Chinese Academy of Sciences, Suzhou 215123, China
e-mail: gbpan2008@sinano.ac.cn

B. He
School of Electrical and Electronic Engineering, Nanyang Technological University, 50 Nanyang Avenue, Singapore 639798, Singapore

S.-H. Zhang
Institute of Microscale Optoelectronics, Shenzhen University, Shenzhen 518060, China

1. Materials

Fresh bamboo leaves (Suzhou Institute of Nano-Tech and Nano-Bionics, China), sodium hydroxide (NaOH, 99%, AR), cerium (III) nitrate hexahydrate ($Ce(NO_3)_3 \cdot 6H_2O$, 99%, AR), gold chloride trihydrate ($HAuCl_4 \cdot 3H_2O$, 99.9%, metals basis) and ethanol (C_2H_5OH, 99%, AR) were used to prepare sensing materials. Except for bamboo leaves, other reagents were commercially available and used without any further purification.

2. Characterization of as-prepared samples

The surface morphology and elemental analysis of as-prepared CQDs and Au/CeO_2@CQDs were determined by scanning electron microscopy (SEM, Hitachi S-4800) and energy dispersive X-ray spectroscopy (EDS, Quanta FEG 250), respectively. The crystal structure of CeO_2@CQDs and Au/CeO_2@CQDs were carried out by X-ray diffraction at a scanning rate of 0.1° s^{-1}, using Cu Kα radiation (XRD, Bruker D8 Advance power X-ray diffractometer). The chemical composition of samples was characterized by X-ray photoelectron spectrometer (ESCALab MKII). The surface morphology, elemental mapping and crystal structure of as-prepared Au/CeO_2@CQDs was also obtained by transmission electron microscopy (TEM) and high-resolution transmission electron microscopy (HRTEM, Tencnai G2 F20 S-TWIN) images, respectively. The size of the CQDs NPs was characterized with a Malvern Zetasizer instrument (Malvern, Zetasizer Nano, UK).

3. Gas sensing test system in different humidity environments

A cylinder of 100 ppm NO_2 (Air Products) balanced by nitrogen was used. Mass flow controllers (MFCs, Sevenstar CS200, China) controlled were employed to dilute the 100 ppm NO_2 in a chamber to desired concentration using air with different humidity, which was controlled by a KickStart software through general purpose interface bus. The mixed gases were delivered to the chamber with a constant flow rate of 400 sccm. Before and after exposure of the sensor to NO_2, the chamber was purged with dry air.

Fig.S1 Schematic diagram of photodeposition of Au NPs.

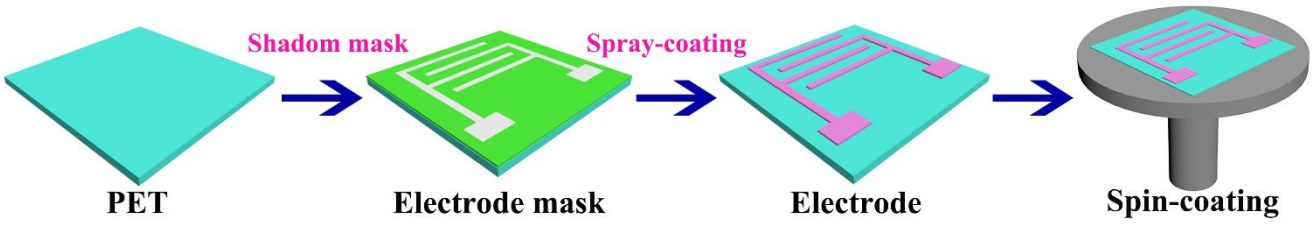

Fig.S2 Schematic illustrations of preparing a PET substrate with Au interdigital electrodes.

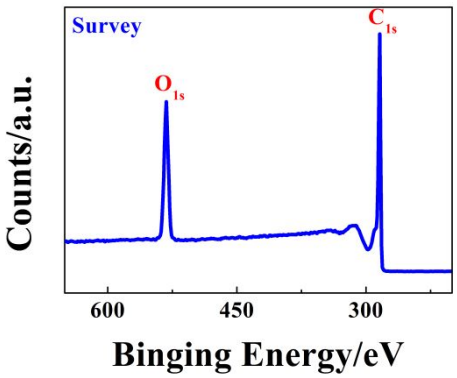

Fig.S3 XPS full survey spectra of CQDs.

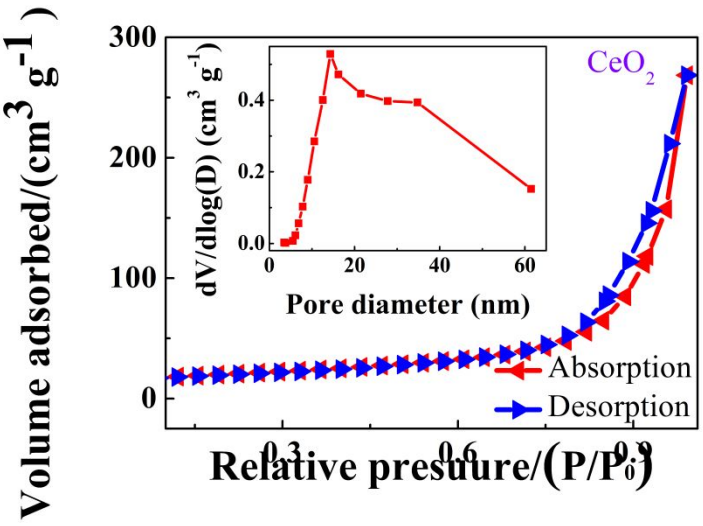

Fig.S4 Nitrogen adsorption−desorption isotherms of pure CeO_2 (the inset plot displays BJH desorption pore-size distribution of pure CeO_2).

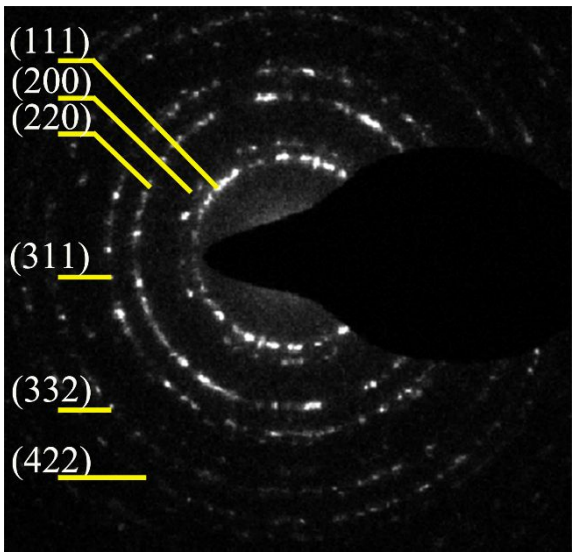

Fig.S5 Selected area electron diffraction (SAED) pattern of CeO_2@CQDs.

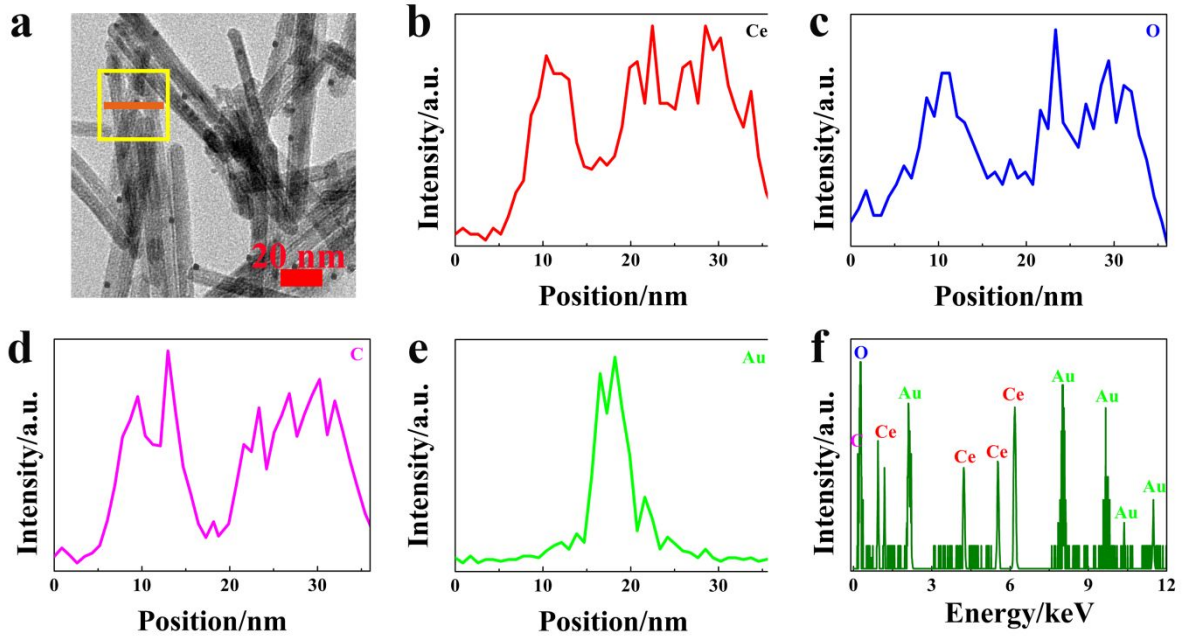

Fig.S6 **a** TEM image of Au/CeO_2@CQDs. **b–e** Line-scan profiles of Ce, O, C and Au element distribution in as-prepared sample corresponding to Figure S6a (marked by red line). **f** EDS spectrum of Au/CeO_2@CQDs.

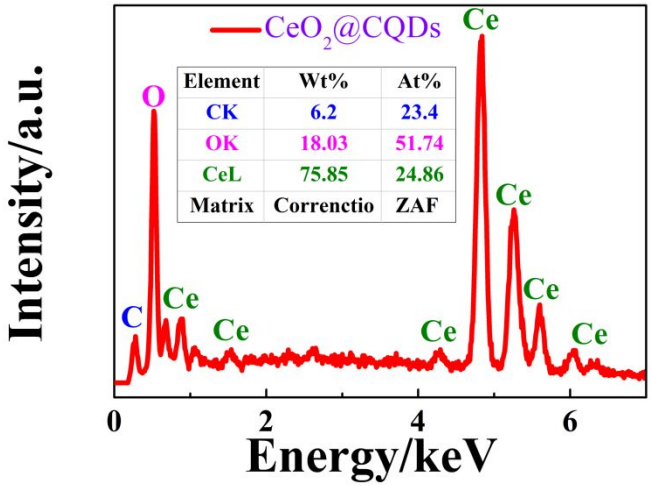

Fig.S7 EDX spectrum of CeO_2@CQDs

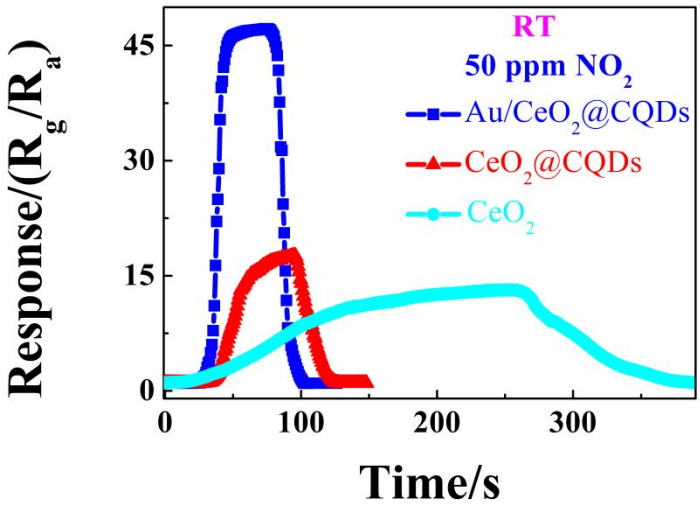

Fig.S8 Response curves of devices based on pure CeO_2, CeO_2@CQDs and Au/CeO_2@CQDs.

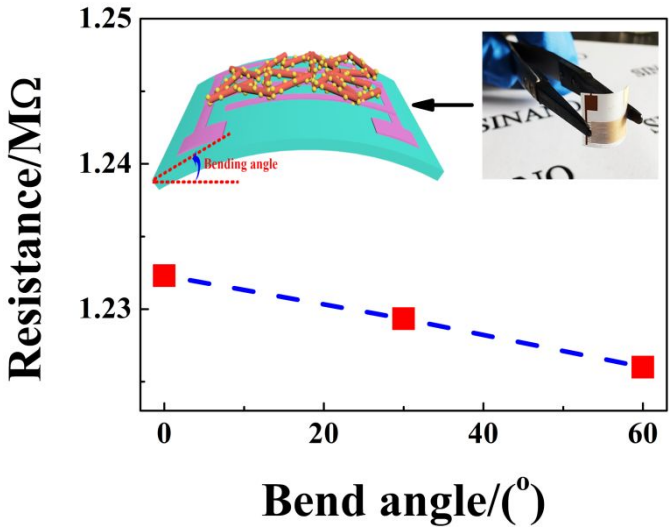

Fig.S9 Flexibility of Au/CeO_2@CQDs gas sensor on PET substrate: The resistance of the sensor in air under different bending angles. Inset: Image of the bent sensor.

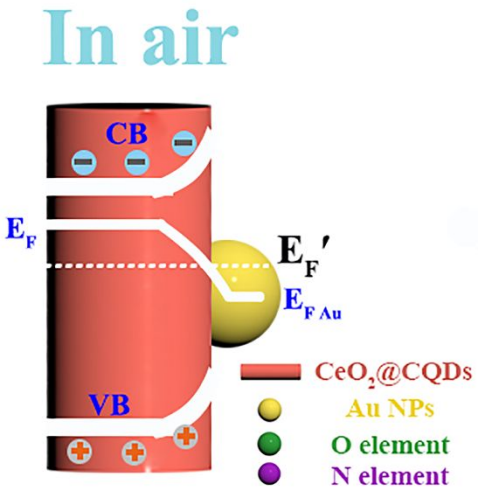

Fig.S10 Schematic presentation of electron transportation of Au/CeO_2@CQDs exposed to air.

Fig.S11 Photograph of gas sensor thickness measurement.

Table S1 NO_2 sensing performance of different sensing materials.

Materials	Gas concentration (ppm)	Sensor reponse (R_a/R_g)	Response time (s)	Recovery time (s)	Operating temperature (°C)	Reference
Au/CeO_2@CQDs	50	47	18	22	RT	**This work**
C-CeO_2nanoparticles	40	2.2	240	438	100	[1]
CeO_2-NiO	125	67.34%	28	54	125	[2]
UV-RGO/CeO_2	10	234	-	258	RT	[3]
Au/Pd@ZNWs	1	210%	35	30	100	[4]
UV-WSe_2	5	35	76	109	RT	[5]
AuPt/$SnSe_2$	8	4.62	82	137	130	[6]
CeO_2/SnO_2	100	37	2	70	225	[7]
CeO_2/graphene	200	48	181	246	RT	[8]

Notes: – means Not reported.

Reference

[1] Oosthuizen D. N., Motaung D. E. and Swart H. C., Gas sensors based on CeO_2 nanoparticles prepared by chemical precipitation method and their temperature-dependent selectivity towards H_2S and NO_2 gases, Applied Surface Science. 2020; 505:144356.https://doi.org/10.1016/j.apsusc.2019.144356.
[2] Kabure A. A., Shirke B. S., Mane S. R. and Garadkar K. M., Microwave-assisted sol-gel synthesis of CeO_2-NiO nanocomposite based NO_2 gas sensor for selective detection at lower operating temperature, Journal of the Indian Chemical Society. 2022; 99(3):100369.https://doi.org/10.1016/j.jics.2022.100369.
[3] Hu J., Zou C., Su Y., Li M., Ye X., Cai B., Kong E. S. W., Yang Z. and Zhang Y., Light-assisted recovery for a highly-sensitive NO_2 sensor based on RGO-CeO_2 hybrids, Sensors and Actuators B: Chemical. 2018; 270:119.https://doi.org/10.1016/j.snb.2018.05.027.
[4] Chen X., Shen Y., Zhou P., Zhong X., Li G., Han C., Wei D. and Li S., Bimetallic Au/Pd nanoparticles decorated ZnO nanowires for NO_2 detection, Sensors and Actuators B: Chemical. 2019; 289.https://doi.org/10.1016/j.snb.2019.03.095.
[5] Lu G. C., Liu X. H., Zheng W., Xie J. Y., Li Z. S., Lou C. M., Lei G. L. and Zhang J., UV-activated single-layer WSe_2 for highly sensitive NO_2 detection, Rare Metals. 2022; 41(5):1520.https://doi.org/10.1007/s12598-021-01899-7.
[6] Liu W., Gu D. and Li X., AuPt bimetal-functionalized $SnSe_2$ microflower-based sensors for detecting sub-ppm NO_2 at low temperatures, ACS Applied Materials & Interfaces. 2021; 13(17):20336.https://doi.org/10.1021/acsami.1c02500.
[7] Liu J., Dai M., Wang T., Sun P., Liang X., Lu G., Shimanoe K. and Yamazoe N., Enhanced gas sensing properties of SnO_2 hollow spheres decorated with CeO_2 nanoparticles heterostructure composite materials, ACS Applied Materials & Interfaces. 2016; 8(10):6669.https://doi.org/10.1021/acsami.6b00169.
[8] Zhang L., Fang Q., Huang Y., Xu K., Chu P. K. and Ma F., Oxygen Vacancy Enhanced Gas-Sensing Performance of CeO_2/Graphene Heterostructure at Room Temperature, Analytical Chemistry. 2018; 90(16).https://doi.org/10.1021/acs.analchem.8b01768.